Supporting Information

Chang et al. 10.1073/pnas.1311760110

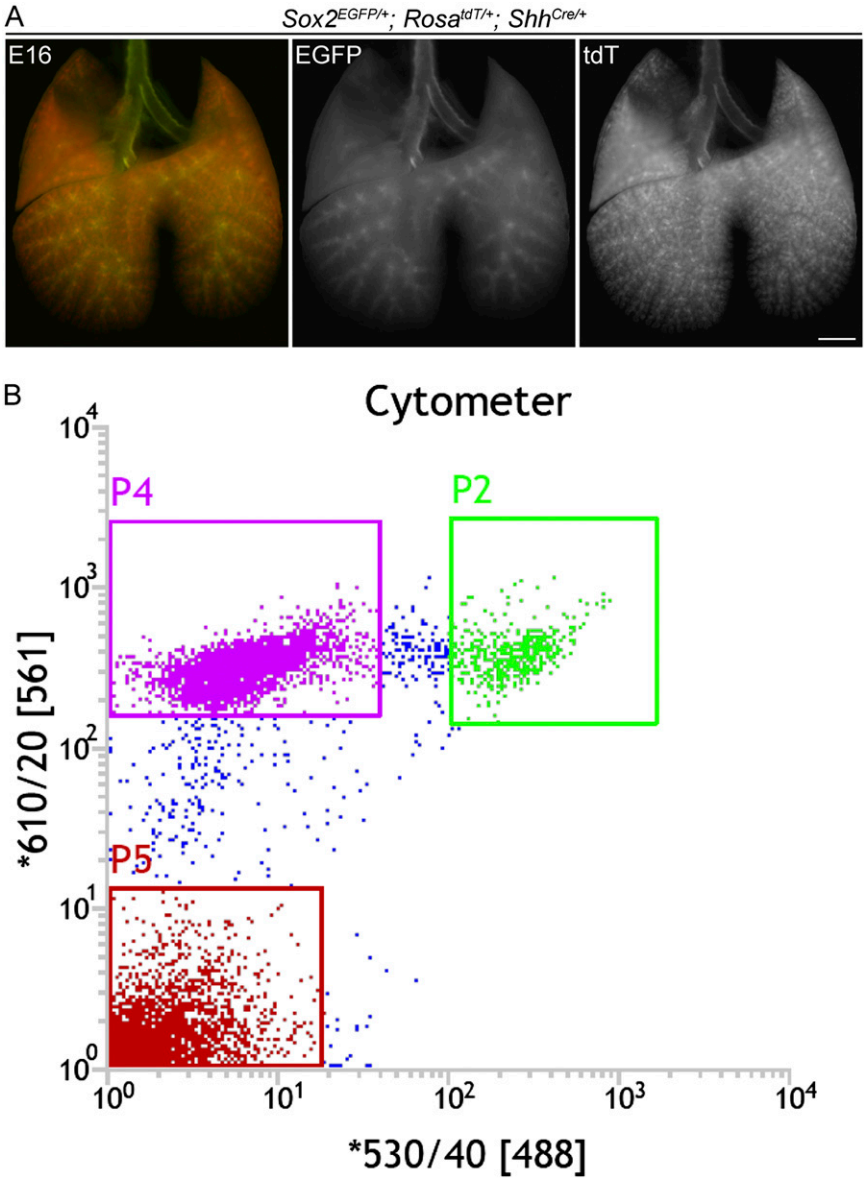

Fig. S1. FACS purification of distal lung epithelial cells. (*A*) Stereoscope images of an embryonic day (E)16 *SRY-box containing gene 2* (*Sox2*)$^{EGFP/+}$;*Rosa*$^{tdT/+}$; *Sonic hedgehog* (*Shh*)$^{Cre/+}$ lung showing that distal epithelial cells express red (tdT), but not green (EGFP), fluorescent proteins. (Scale bar, 500 μm.) (*B*) A representative FACS graph of E17 *Sox2*$^{EGFP/+}$;*Rosa*$^{tdT/+}$;*Shh*$^{Cre/+}$ lungs showing separation of distal epithelial cells (P4 fraction) from proximal epithelial cells (P2 fraction) and nonepithelial cells (P5 fraction).

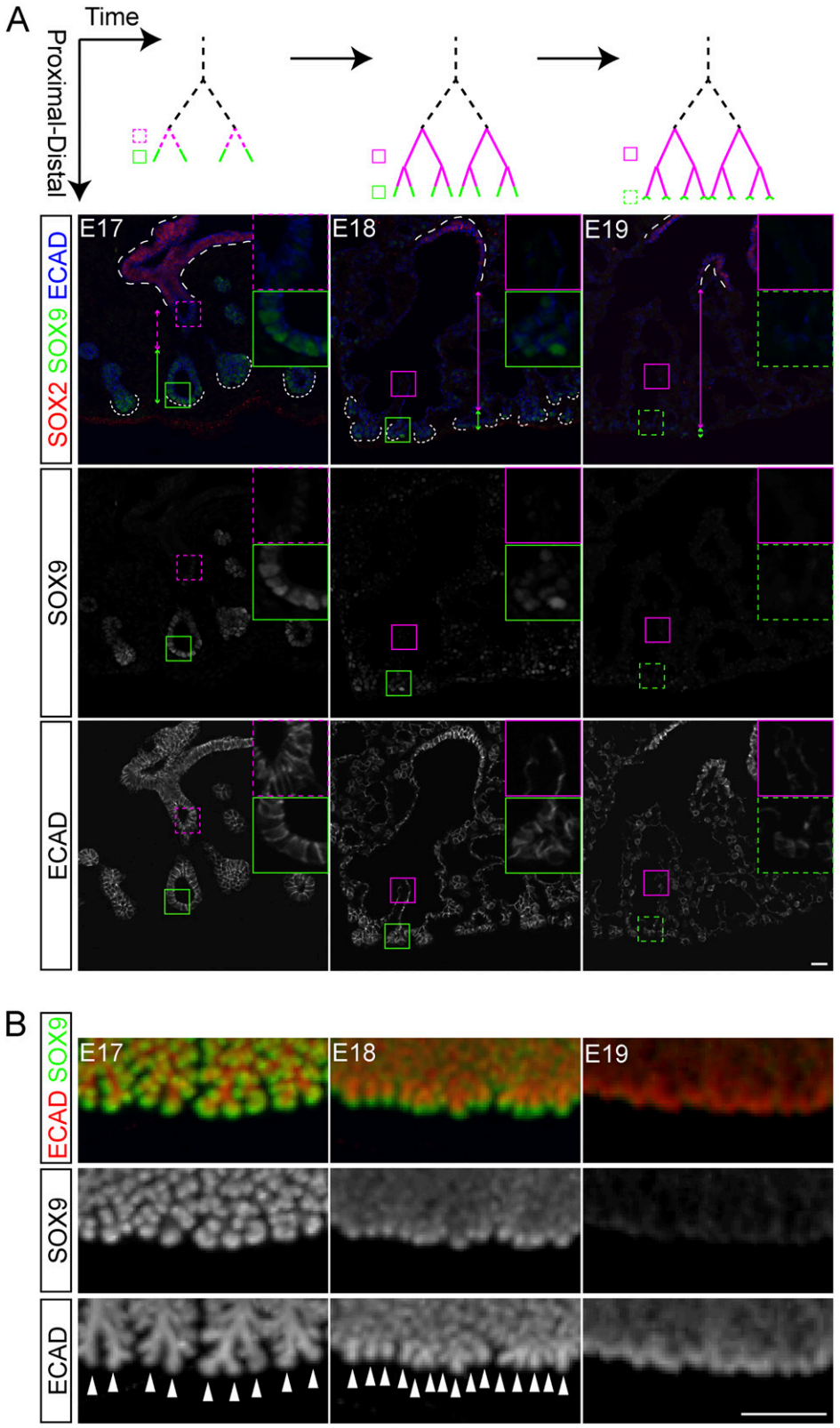

Fig. S2. Branching program in late lung development. (*A*) Confocal images of immunostained lung sections in areas where the airway lumen can be continuously traced from the proximal conducting airways (black/white long dashed lines) to the distal nonbranch tip (magenta) and branch tip (green) regions, as illustrated in the schematics. SOX9^{+} branch tips are present near the distal edges of E17–E19 lungs. Branch tips are outlined with dashed lines at E17–E18 and are too small to be completely captured on sections at E19. The boxed regions are enlarged (*Insets*) outlined in corresponding colors. Dashed magenta and green boxes indicate a low level of alveolar differentiation (Fig. S3) and branching, respectively. The images for E18 lungs are replicated from Fig. 1*B*. (Scale bar, 20 μm.) (*B*) Optical projection tomography (OPT) images of the distal edges of whole mount immunostained lungs showing an increase in the number of SOX9^{+} branch tips from E17 to E18 (arrowheads). Very few cells at the branch tips express SOX9. (Scale bar, 250 μm.)

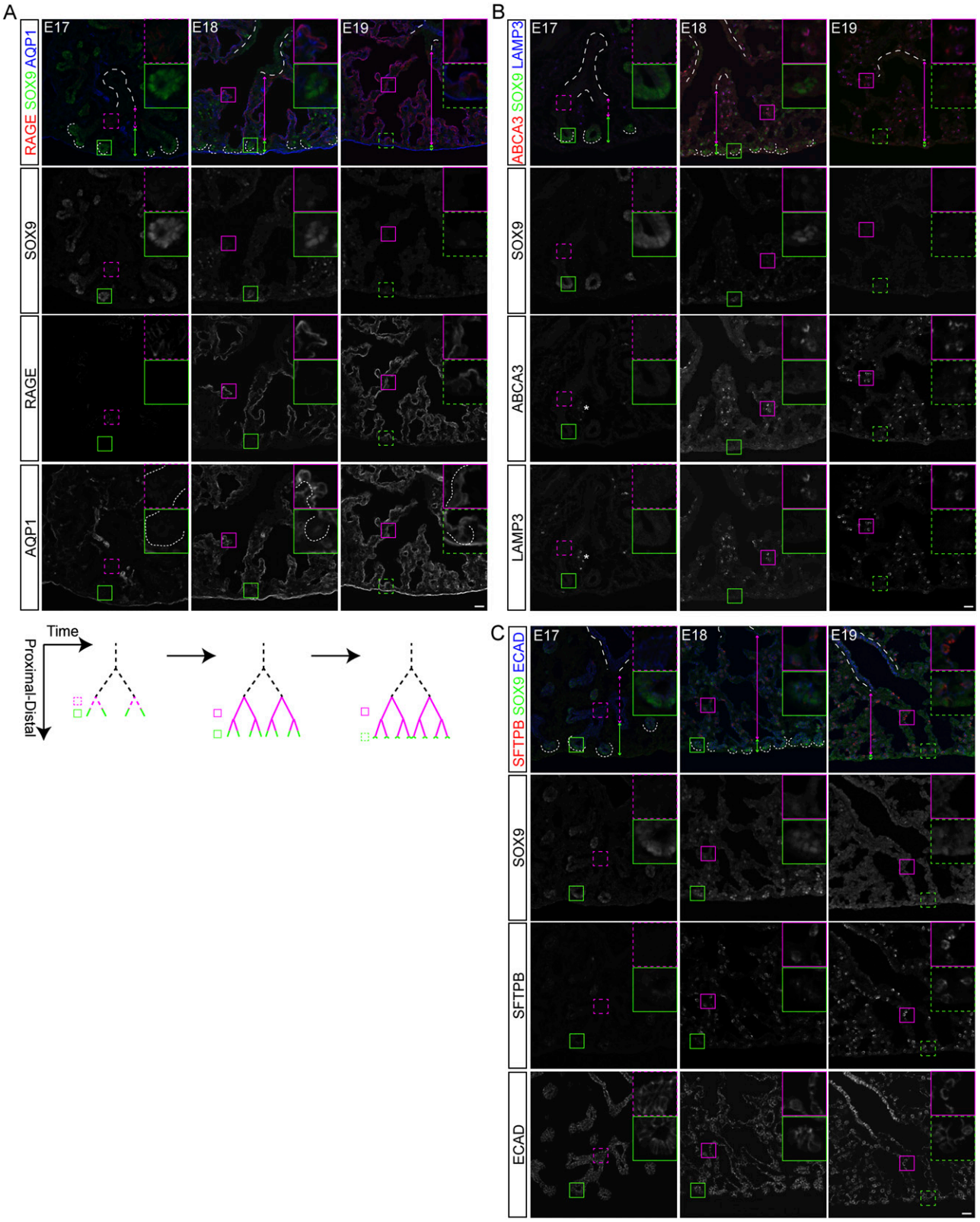

Fig. S3. Temporal progression and proximal/distal distribution of the alveolar differentiation program. Confocal images of immunostained lung sections in areas where the airway lumen can be continuously traced from the proximal conducting airways (black/white long dashed lines) to the distal nonbranch tip (magenta) and branch tip (green) regions, as illustrated in the schematics. Differentiation of alveolar type I [Aquaporin 1 (AQP1) and receptor for advanced glycosylation of end products (RAGE) in *A*] and type II [ABCA3 and LAMP3 in *B* and *Surfactant protein B* (SFTPB) in *C*] cells occurs in nonbranch tip regions of the distal epithelium and expands distally at E19 when the branch tips consist of a few $SOX9^{+}$ cells. Branch tips are outlined with dashed lines at E17–E18 and are too small to be completely captured on sections at E19. The boxed regions are enlarged as insets outlined in corresponding colors. Dashed magenta and green boxes indicate a low level of alveolar differentiation and branching, respectively. AQP1 labels alveolar type I cells, the vasculature, and the mesothelium, which are separated by dashed lines in the insets. The images for E18 lungs are replicated from Fig. 1*B*. Asterisks in *B* indicate autofluorescence from blood cells. (Scale bars, 20 μm.)

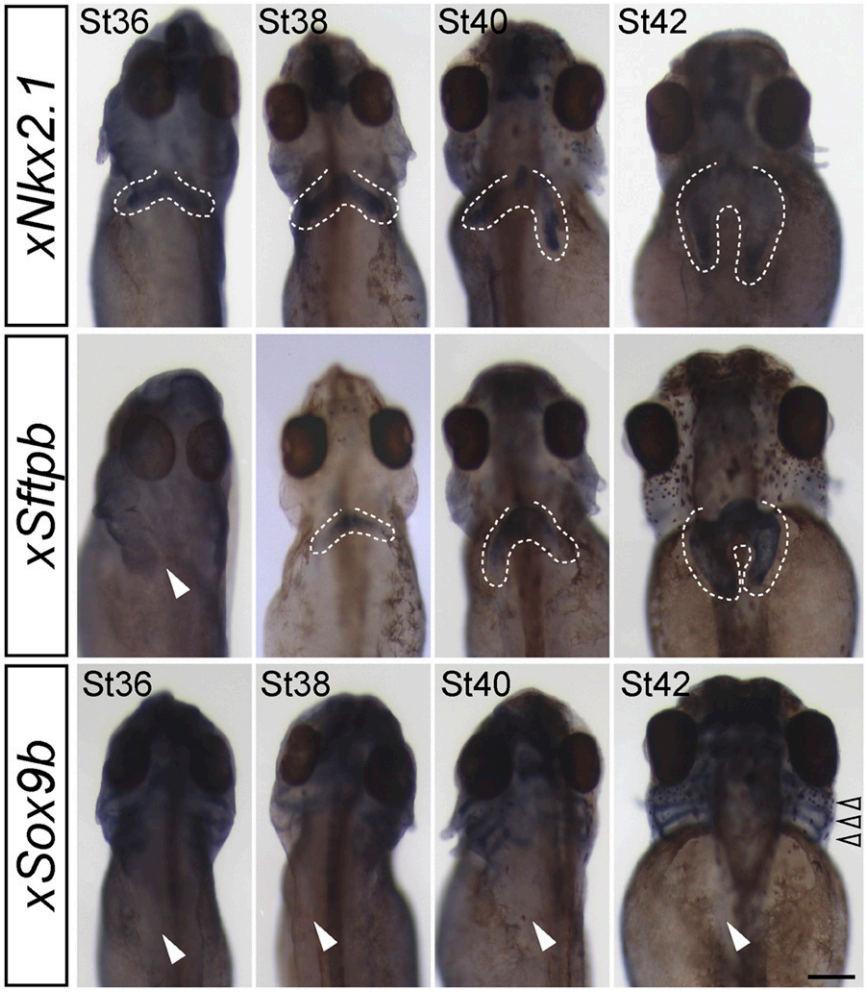

Fig. S4. *Xenopus* lungs lack the branching program and *Sox9* expression, and initiates alveolar differentiation immediately after lung specification. Whole mount in situ hybridization of *Xenopus* embryos at indicated stages (St). The lungs are indicated with dashed lines if stained or arrowheads if unstained. Open arrowheads indicate *Sox9* expression in the pharyngeal arches. The onset of *Sftpb* expression is slightly later than that of *Sftpc* expression (Fig. 1*C*). (Scale bar, 200 μm.)

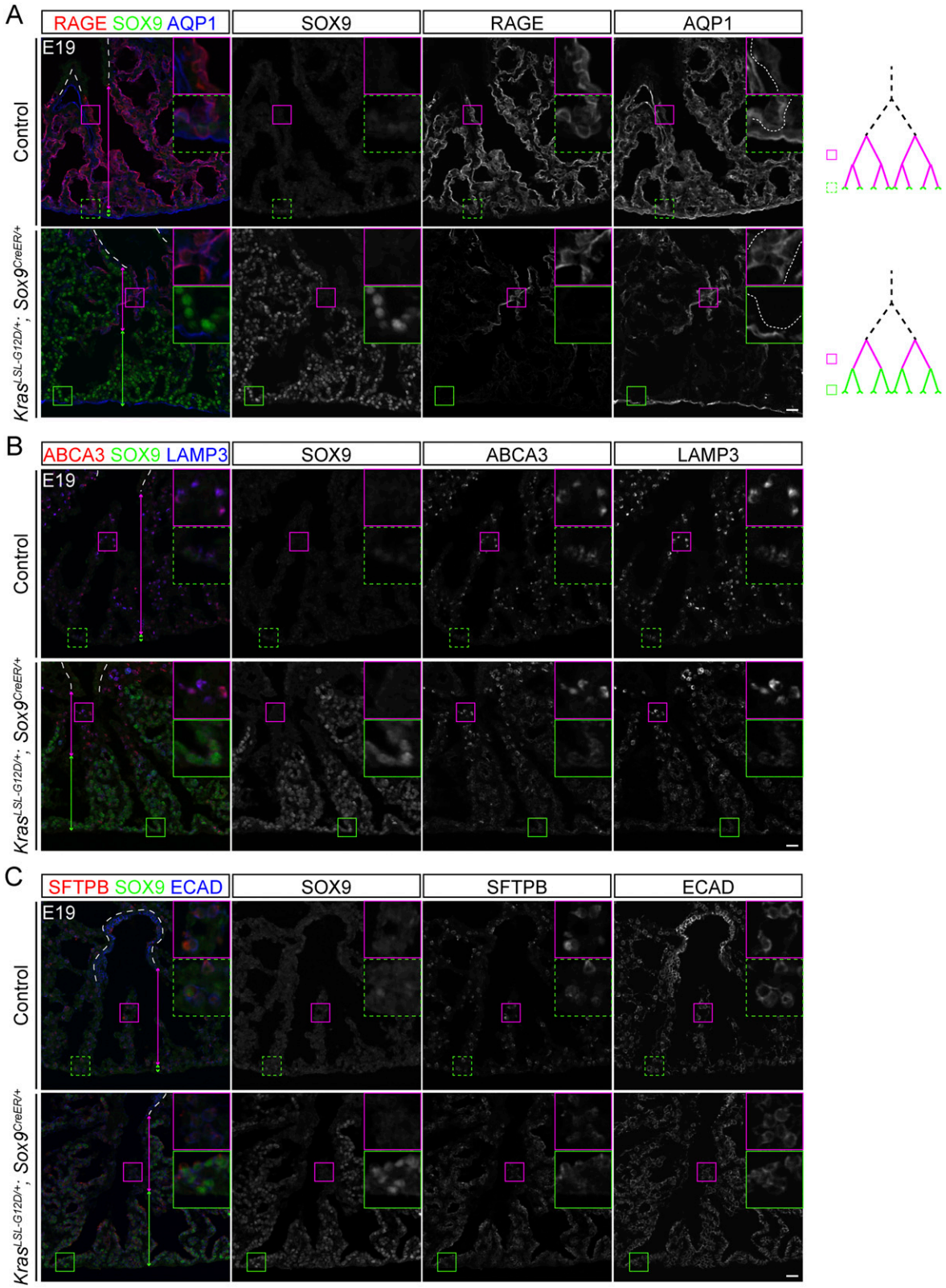

Fig. S5. Hyperactive *Kras* suppresses alveolar differentiation. Confocal images of immunostained lung sections in areas where the airway lumen can be continuously traced from the proximal conducting airways (black/white long dashed lines) to the distal nonbranch tip (magenta) and branch tip (green) regions, as illustrated in the schematics. Expression of alveolar type I (AQP1 and RAGE in *A*) and type II (ABCA3 and LAMP3 in *B*) markers is restricted to nonbranch tip regions closer to the conducting airways in the *Kras* mutant lung. Although SFTPB expression is more uniform in the *Kras* mutant, cells in the expanded branching regions are more clustered as shown by ECAD (E-cahedrin) staining (*C*). The boxed regions are enlarged (*Insets*) outlined in corresponding colors. Dashed green boxes indicate a low level of branching with a few SOX9-positive cells. (Scale bars, 20 μm.)

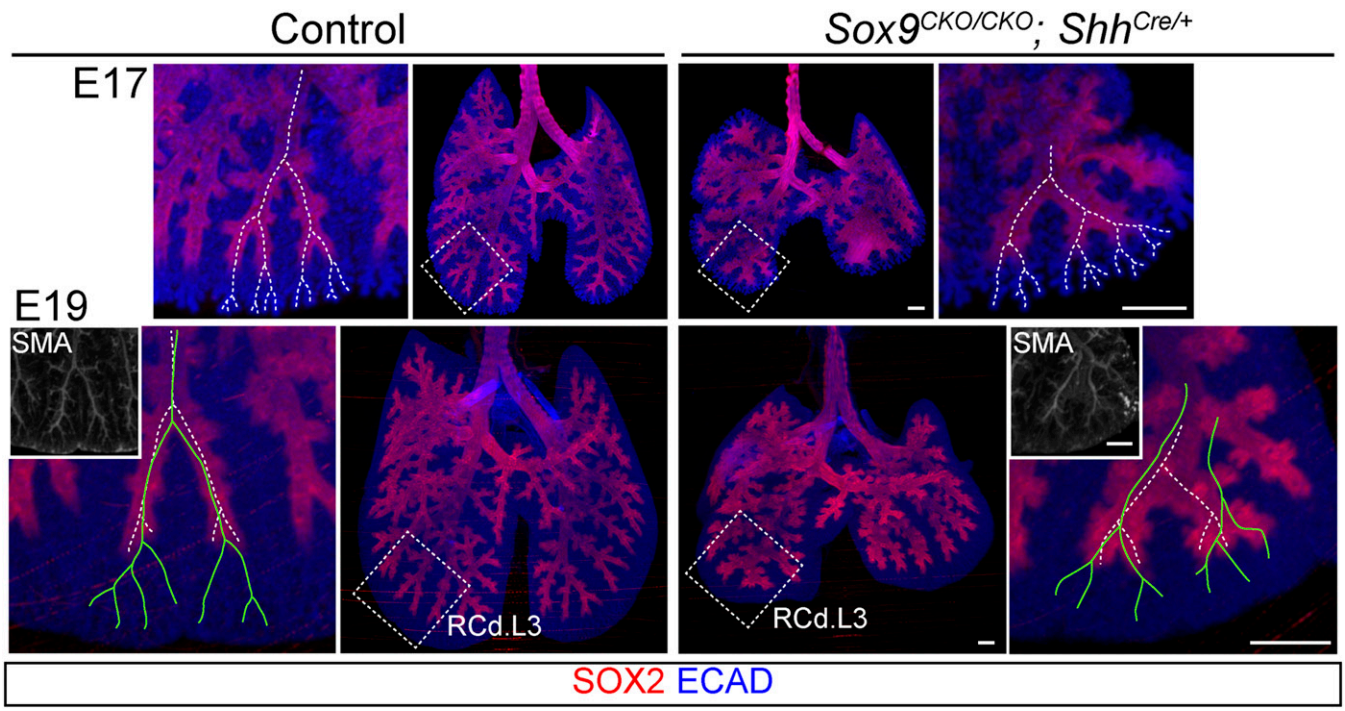

Fig. S6. Persistent branching defects and normal coalignment between airway branches and arteries in the *Sox9* mutant lung. OPT images of whole-mount immunostained lungs from littermate control (*Left*) and $Sox9^{CKO/CKO};Shh^{Cre/+}$ mutant (*Right*) embryos. The RCd.L3 branch lineages (1) in the boxed areas are enlarged and traced with dashed lines. Only the $SOX2^{+}$ branches are traced for E19. The arteries in E19 lungs immunostained for smooth muscle actin (SMA) are identified by their connection to the main pulmonary arteries, traced with solid green lines and shown (*Insets*). (Scale bars, 250 μm.)

1. Metzger RJ, Klein OD, Martin GR, Krasnow MA (2008) The branching programme of mouse lung development. *Nature* 453(7196):745–750.

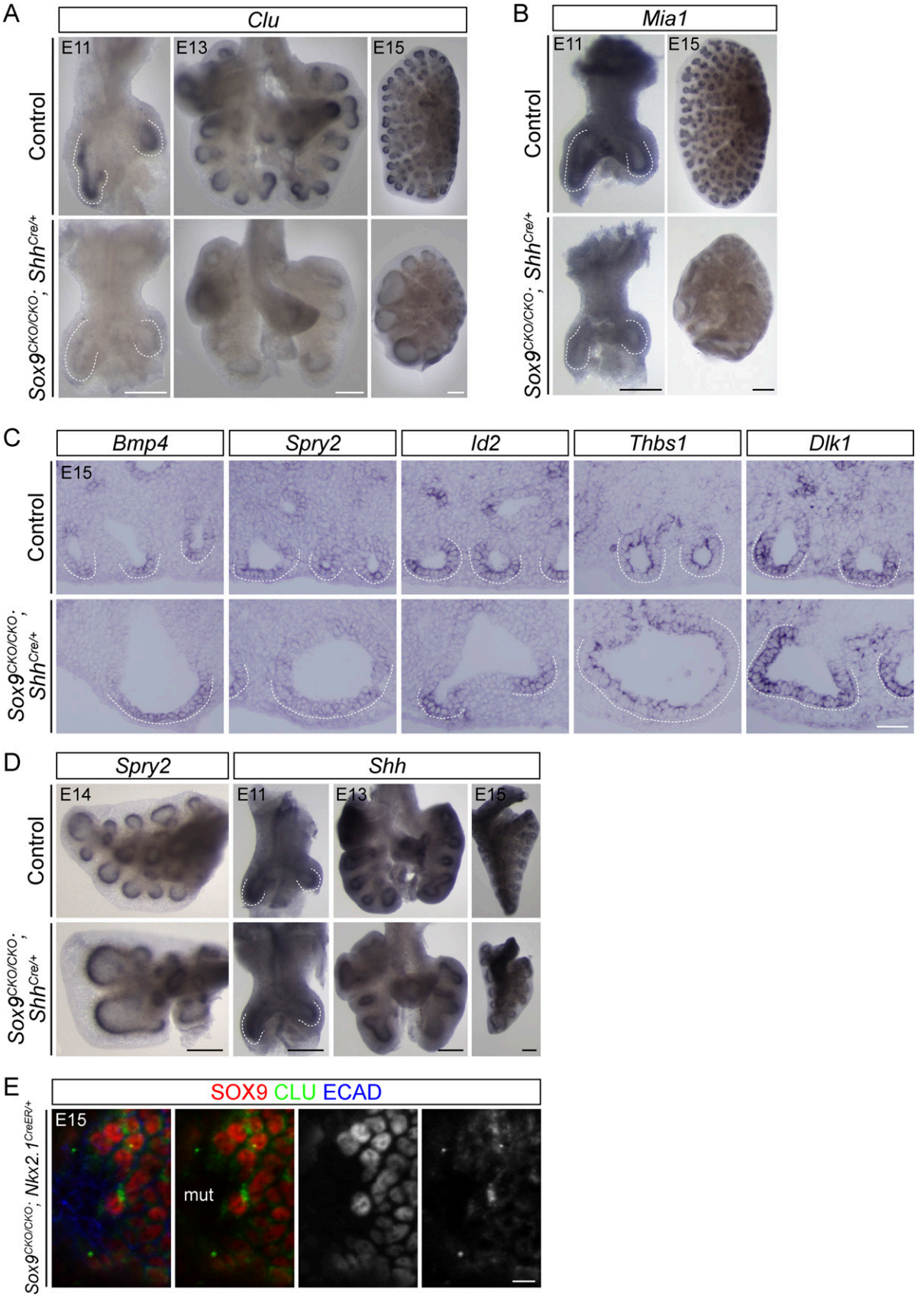

Fig. S7. *Sox9*-dependent and -independent branching related genes. Whole-mount (*A*, *B*, and *D*) and section (*C*) in situ hybridization of littermate control and $Sox9^{CKO/CKO};Shh^{Cre/+}$ mutant lungs. Expression of *Clusterin* (*Clu*) and *Melanoma inhibitory activity 1* (*Mia1*) is dependent on *Sox9*, whereas expression of *Bmp4*, *Spry2*, *Id2*, *Thbs1*, *Dlk1*, and *Shh* is independent of *Sox9*. Branch tips are traced with dashed lines. [Scale bars, 200 μm (*A*, *B*, *D*) and 50 μm (*C*).] (*E*) Projection images of an E15 whole-mount immunostained $Sox9^{CKO/CKO};Nkx2.1^{CreER/+}$ mutant lung showing the absence of CLU in $SOX9^{-}$ cells (mut). (Scale bar, 10 μm.)

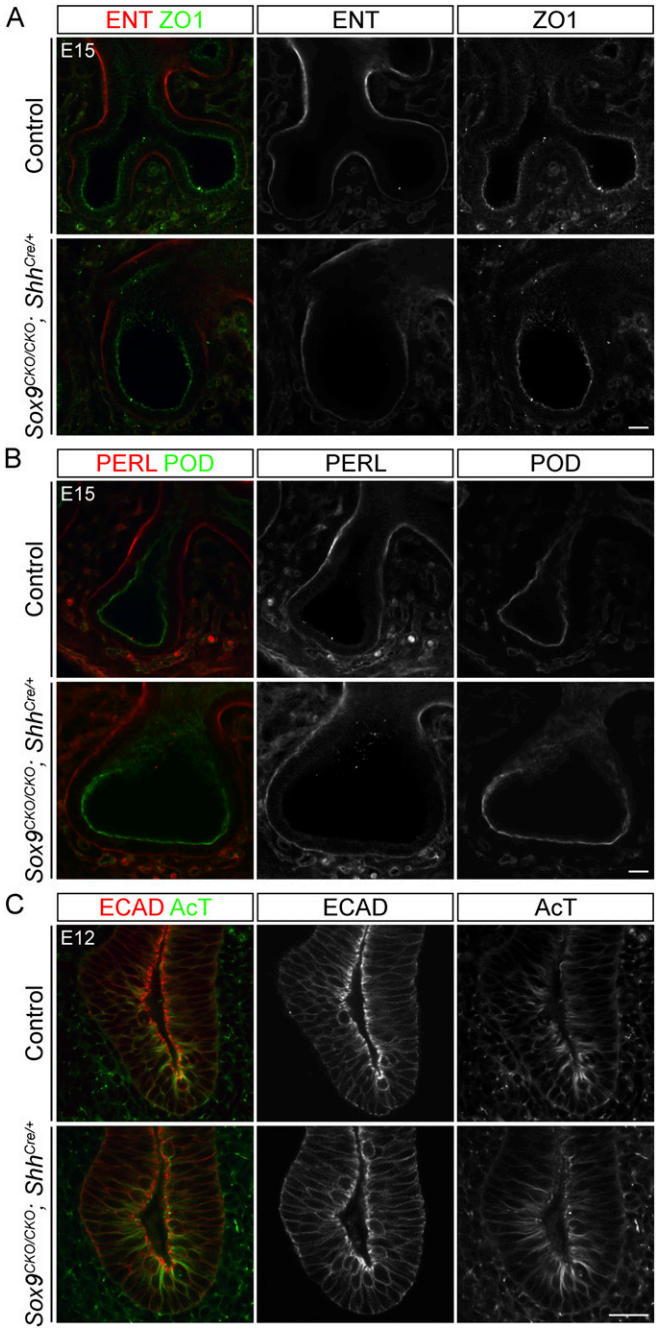

Fig. S8. Normal cell polarity in the *Sox9* mutant lung. Confocal images of whole mount immunostained E15 (*A* and *B*) and E12 (*C*) littermate control and $Sox9^{CKO/CKO}$;$Shh^{Cre/+}$ mutant lungs. The *Sox9* mutant lung has no significant change in the distribution of apical [Zonula occluden 1 (ZO1) and Podocalyxin-like (POD)], basement membrane [Entactin (ENT) and Perlecan (PERL)] and cytoskeleton [acetylated Tubulin (AcT)] markers. (Scale bars, 20 μm.)

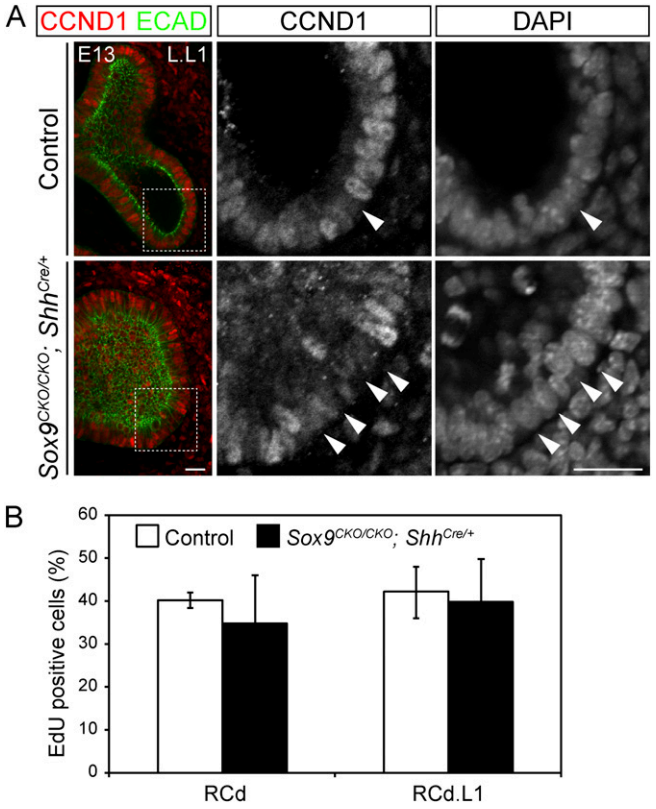

Fig. S9. Cell proliferation in the *Sox9* mutant lung. (*A*) Confocal images of the L.L1 branch lineage (1) of E13 whole-mount lungs from littermate control and $Sox9^{CKO/CKO};Shh^{Cre/+}$ mutant embryos, immunostained for ECAD and Cyclin D1 (CCND1). The boxed areas are enlarged in subsequent panels. Arrowheads indicate cells expressing a very low level of CCND1 [2% in control lungs ($n = 293$) versus 11% in *Sox9* mutant lungs ($n = 252$), $P < 0.001$, χ^2 test]. (Scale bar, 20 μm.) (*B*) The percentages of 5-ethynyl-2′-deoxyuridine $(EdU)^+$ cells in the RCd lobar and RCd.L1 (1) branch tips are not significantly different between E14 littermate control and $Sox9^{CKO/CKO};Shh^{Cre/+}$ mutant lungs ($P > 0.05$, Student *t* test). Error bars represent SDs.

1. Metzger RJ, Klein OD, Martin GR, Krasnow MA (2008) The branching programme of mouse lung development. *Nature* 453(7196):745–750.

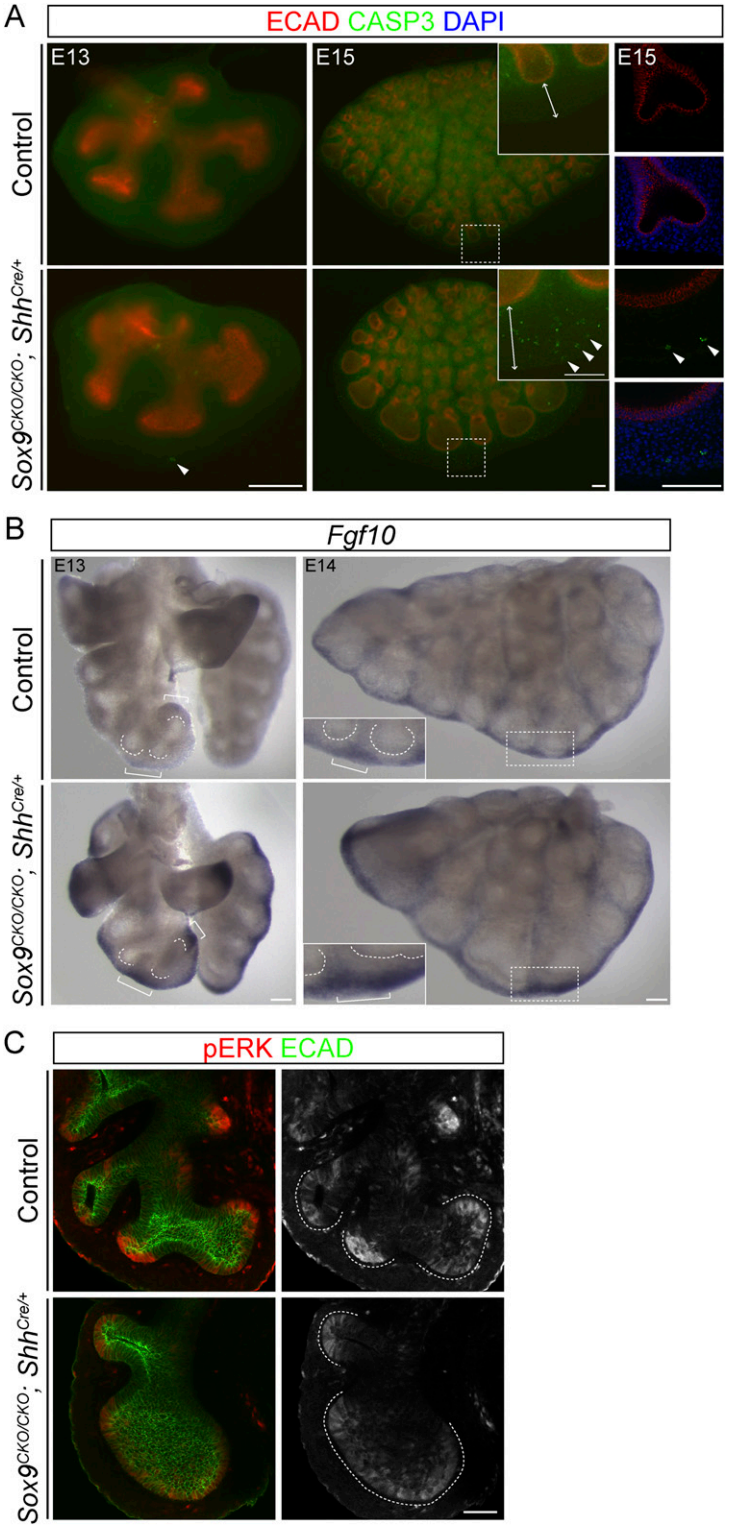

Fig. S10. *Sox9* regulates mesenchymal cell survival and *Fgf10* signaling. (*A*) Stereoscope images of whole-mount lungs from littermate control and $Sox9^{CKO/CKO}$; $Shh^{Cre/+}$ mutant embryos, immunostained for ECAD, cleaved Caspase-3 (CASP3), and DAPI. The boxed areas are enlarged (*Insets*). The number of apoptotic cells in the mesenchyme of the $Sox9^{CKO/CKO}$;$Shh^{Cre/+}$ mutant lungs increases from E13 to E15 (arrowheads). Confocal images of the E15 lungs are shown in the rightmost column. Compared with the confocal images, the stereoscope images are a projection view of the whole lung and therefore have more background autofluorescence and more apoptotic cells. Double-headed arrows indicate the increased distance between the epithelium and the mesothelium in the *Sox9* mutant lung. (Scale bars, 100 μm.) (*B*) *Fgf10* whole mount in situ hybridization of littermate control and $Sox9^{CKO/CKO}$;$Shh^{Cre/+}$ mutant lungs. The boxed areas are shown as insets. Square brackets indicate increased *Fgf10* expression in the *Sox9* mutant lung. Branch tips are traced with dashed lines. (Scale bar, 100 μm.) (*C*) Confocal images of E13 whole-mount littermate control and $Sox9^{CKO/CKO}$;$Shh^{Cre/+}$ mutant lungs, immunostained for phosphorylated extracellular signal-regulated kinase (pERK) and ECAD. pERK staining appears more diffuse in the *Sox9* mutant lung. Branch tips are traced with dashed lines. (Scale bar, 50 μm.)

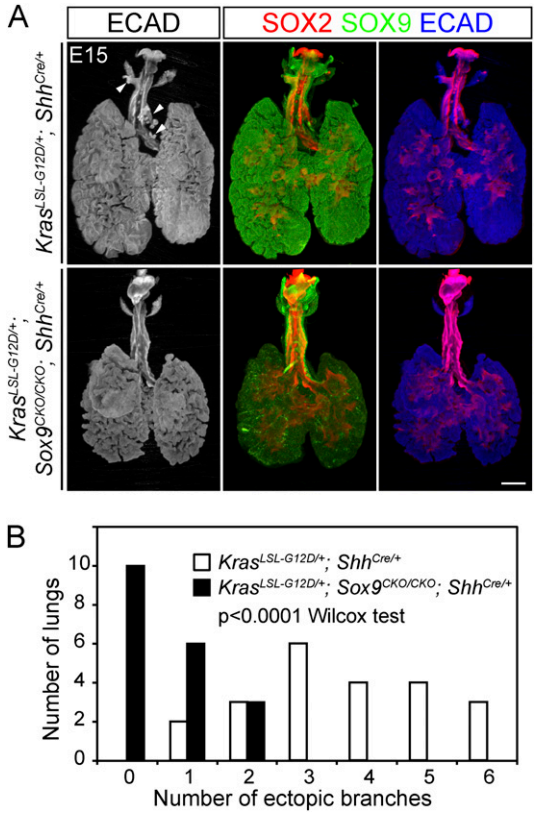

Fig. S11. Epithelial deletion of *Sox9* suppresses ectopic branches in the *Kras* mutant lung. (*A*) OPT images of whole-mount immunostained E15 littermate $Kras^{LSL\text{-}G12D/+};Shh^{Cre/+}$ mutant and $Kras^{LSL\text{-}G12D/+};Sox9^{CKO/CKO};Shh^{Cre/+}$ mutant lungs. Ectopic branches in the $Kras^{LSL\text{-}G12D/+};Shh^{Cre/+}$ mutant lung continue to grow from E13 (Fig. 4*B*) to E15 (arrowheads), but are suppressed by epithelial deletion of *Sox9*. (Scale bar, 500 μm.) (*B*) There is a significant difference ($P < 0.0001$, Wilcoxon test) in the frequency distributions of ectopic branches formed on tracheal and extrapulmonary left/right main bronchial epithelia between E13 $Kras^{LSL\text{-}G12D/+};Shh^{Cre/+}$ (open column) and $Kras^{LSL\text{-}G12D/+};Sox9^{CKO/CKO};Shh^{Cre/+}$ (filled column) mutant lungs. No ectopic branches are present in either control or $Sox9^{CKO/CKO};Shh^{Cre/+}$ mutant lungs.

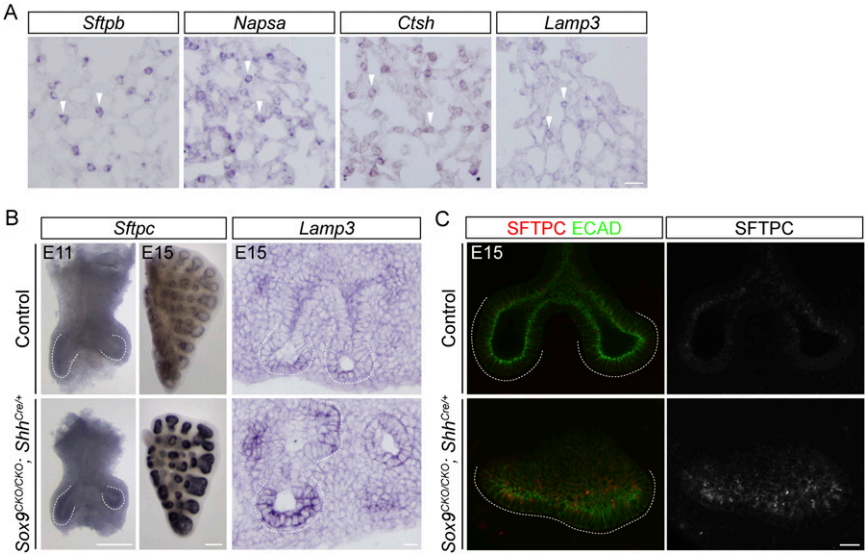

Fig. S12. Precocious initiation of alveolar differentiation in the *Sox9* mutant lung. (*A*) Section in situ hybridization of an adult lung for indicated genes. Arrowheads indicate expression in alveolar type II cells. (Scale bar, 20 μm.) (*B*) Whole-mount (*Sftpc*) (Scale bar, 200 μm) and section (*Lamp3*) (Scale bar, 20 μm) in situ hybridization of littermate control and $Sox9^{CKO/CKO};Shh^{Cre/+}$ mutant lungs. Branch tips are traced with dashed lines. We note that *Sftpc* is expressed at a low level in the control lung and up-regulated in the *Sox9* mutant lung. (*C*) Confocal images of whole-mount immunostained littermate control and $Sox9^{CKO/CKO};Shh^{Cre/+}$ mutant lungs. Branch tips are traced with dashed lines. (Scale bar, 20 μm.)

Dataset S1. Microarray expression profiling of FACS-purified distal lung epithelial cells from E14 through E19

Dataset S1

The original expression values are converted to a $\log_2$ scale when comparing with baseline expression at E14. The two experiments are biological repeats using lungs from independent litters.

Dataset S2. Microarray expression comparison between littermate control and *Sox9*$^{CKO/CKO}$;*Shh*$^{Cre/+}$ mutant lungs at E13, E14, and E15

Dataset S2

The original expression values are converted to a $\log_2$ scale when comparing control and *Sox9* mutant lungs. The two experiments are biological repeats using lungs from independent litters.